Mem. Natl Inst. Polar Res., Spec. Issue, **53**, 109-136, 1998

GENESIS OF THE MIGMATITES OF BREIDVÅGNIPA, EAST ANTARCTICA

Toshiaki SHIMURA[1], Geoffrey L. FRASER[2], Noriyoshi TSUCHIYA[3] and Hiroo KAGAMI[1]

[1]*Graduate School of Science and Technology, Niigata University, 8050, Ikarashi 2-nocho, Niigata 950-2181*
[2]*Department of Geology and Geophysics, University of Adelaide, South Australia, 5005, Australia*
[3]*Department of Geoscience and Technology, Graduate School of Engineering, Tohoku University, Sendai 980-8579*

Abstract: Various types of migmatites and peraluminous granites are widely distributed at Breidvågnipa, which is situated in the granulite-facies part of the Lützow-Holm Complex (LHC) on the eastern coast of Lützow-Holm Bay, East Antarctica. The migmatites consist of paleosome, melanosome, and leucosome, and are intimately associated with peraluminous granite. Modes of field occurrence and petrological features are consistent with the paleosome, melanosome, and leucosome and granite representing original rock, restite, and melt, respectively. The migmatites at Breidvågnipa are therefore regarded as the result of partial melting of pelitic metamorphic rocks during high-grade metamorphism in the LHC.

Thermobarometric calculations indicate peak pressure and temperature conditions at Breidvågnipa of ~0.8 GPa and 870°C. The age of the high-grade metamorphic event is estimated at ~570 Ma, on the basis of a Rb-Sr whole rock isochron from the migmatite. This age is consistent with previously reported U-Pb zircon ages from the LHC.

key words: migmatite, granulite-facies, pertial melting, Lützow-Holm Complex, Rb-Sr isochron age

1. Introduction

The genesis of migmatite has been the subject of considerable research since the early 1900's (*e.g.* SEDERHORM, 1907; MEHNERT, 1968; ATHERTON and GRIBBLE, 1983; ASHWORTH, 1985; JOHANNES *et al.*, 1995). In general, migmatites are present in low P/T type or sometimes in medium P/T type metamorphic belts. A variety of mechanisms have been proposed by different authors to account for production of migmatites, including: (a) metamorphic differentiation, (b) partial melting, (c) injection of granitic magma, (d) assimilation, (e) metasomatism, (f) deformation, (g) crystallization of magma. Migmatites from a particular area may be produced by several of these mechanisms. For example, in the Hidaka Metamorphic Belt of Japan, migmatites were formed by (a), (c), and (e) in the greenschist-facies to lower amphibolite-facies zone, by (a), (b), (d), and (e) in the upper

amphibolite-facies zone, and by (b) and (d) in the granulite-facies zone (SHIMURA *et al.*, 1997).

Here we describe the occurrence and chemical features of the migmatites and granites at Breidvågnipa, East Antarctica, and discuss their origin. We also present data constraining the pressure-temperature conditions, and the age, of metamorphism at Breidvågnipa. In this paper, migmatite terms (*e.g.* paleosome, melanosome, leucosome, agmatic, and stromatic) are after MEHNERT (1968). Mineral abbreviations are after KRETZ (1983) and MIYASHIRO (1994).

2. Geological Outline of Breidvågnipa

Breidvågnipa (69°19′S–69°23′S latitude and 39°44′E–39°52′E longitude) is one of numerous outcrops along the east coast of Lützow-Holm Bay, East Antarctica, and lies

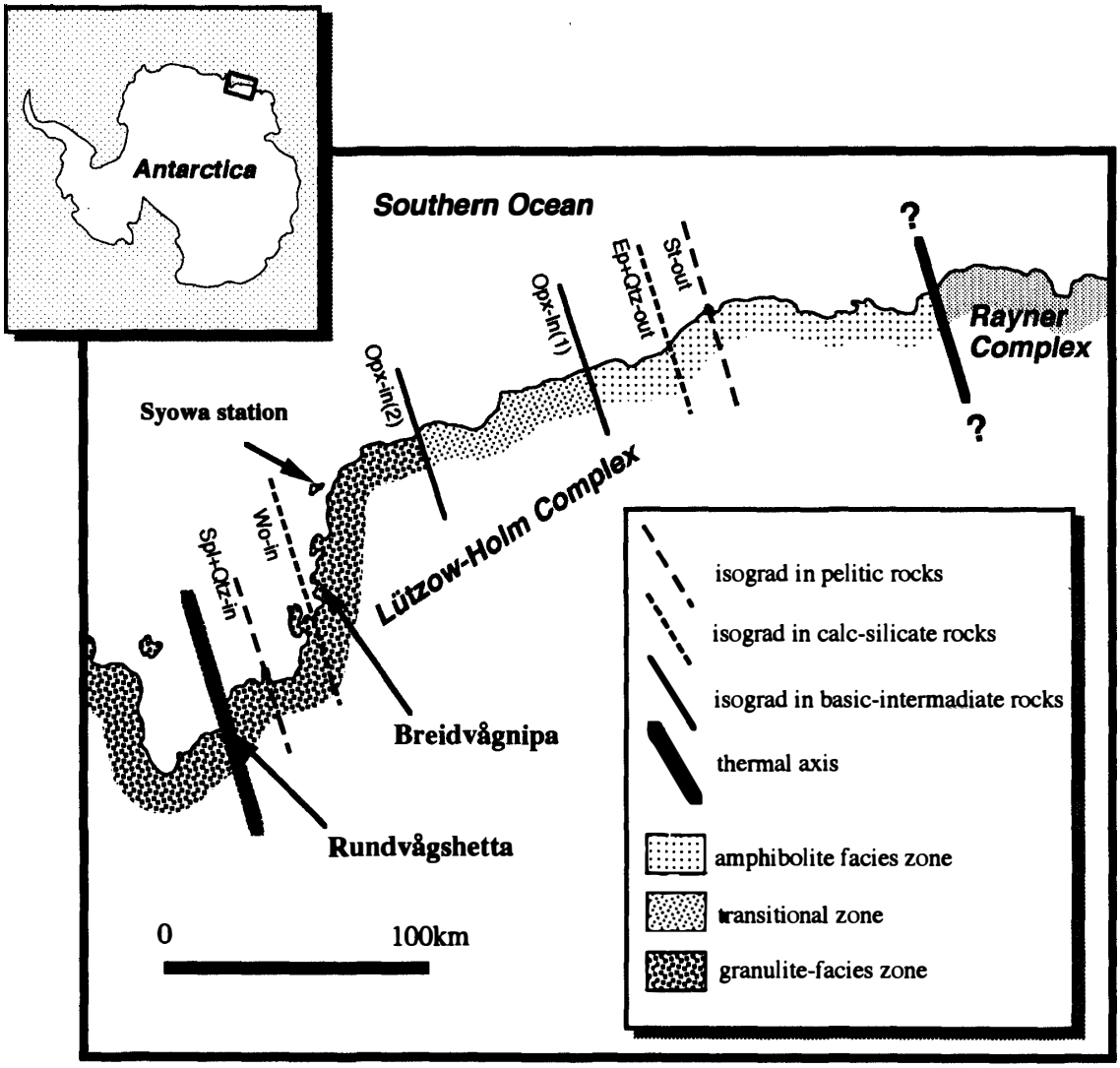

Fig. 1. Locality map of the study area. Metamorphic facies boundaries and isograds are after HIROI *et al. (1989).*

within the granulite-facies portion of the Lützow-Holm Complex (LHC) (SHIRAISHI *et al.*, 1987; HIROI *et al.*, 1991). Metamorphism in the LHC is medium pressure-type and the metamorphic grade increases progressively south-westward from amphibolite- to granulite-facies (MOTOYOSHI *et al.*, 1989; SHIRAISHI *et al.*, 1987; HIROI *et al.*, 1991) (Fig. 1). A clockwise *P-T* evolution has been documented for rocks from throughout the complex (SHIRAISHI *et al.*, 1987; HIROI *et al.*, 1991). The highest grade rocks of the LHC occur at Rundvågshetta, in the southern part of Lützow-Holm Bay, where peak *P-T* conditions reached 1 GPa and ~1000°C (MOTOYOSHI and ISHIKAWA, 1998).

Isotopic ages from the LHC, using a variety of techniques, have been reported by several authors (*e.g.* SHIBATA *et al.*, 1986; SHIRAISHI *et al.*, 1994; FRASER and MCDOUGALL, 1995). SHIRAISHI *et al.* (1994) interpret ion-microprobe U-Pb zircon ages to indicate upper amphibolite to granulite-facies metamorphism occurred during the "Pan African" orogeny, between ~520 and 550 Ma. This interpretation is supported by further zircon dating (FRASER *et al.*, 1997).

Geological surveys in the LHC have been carried out since 1957 by Japanese

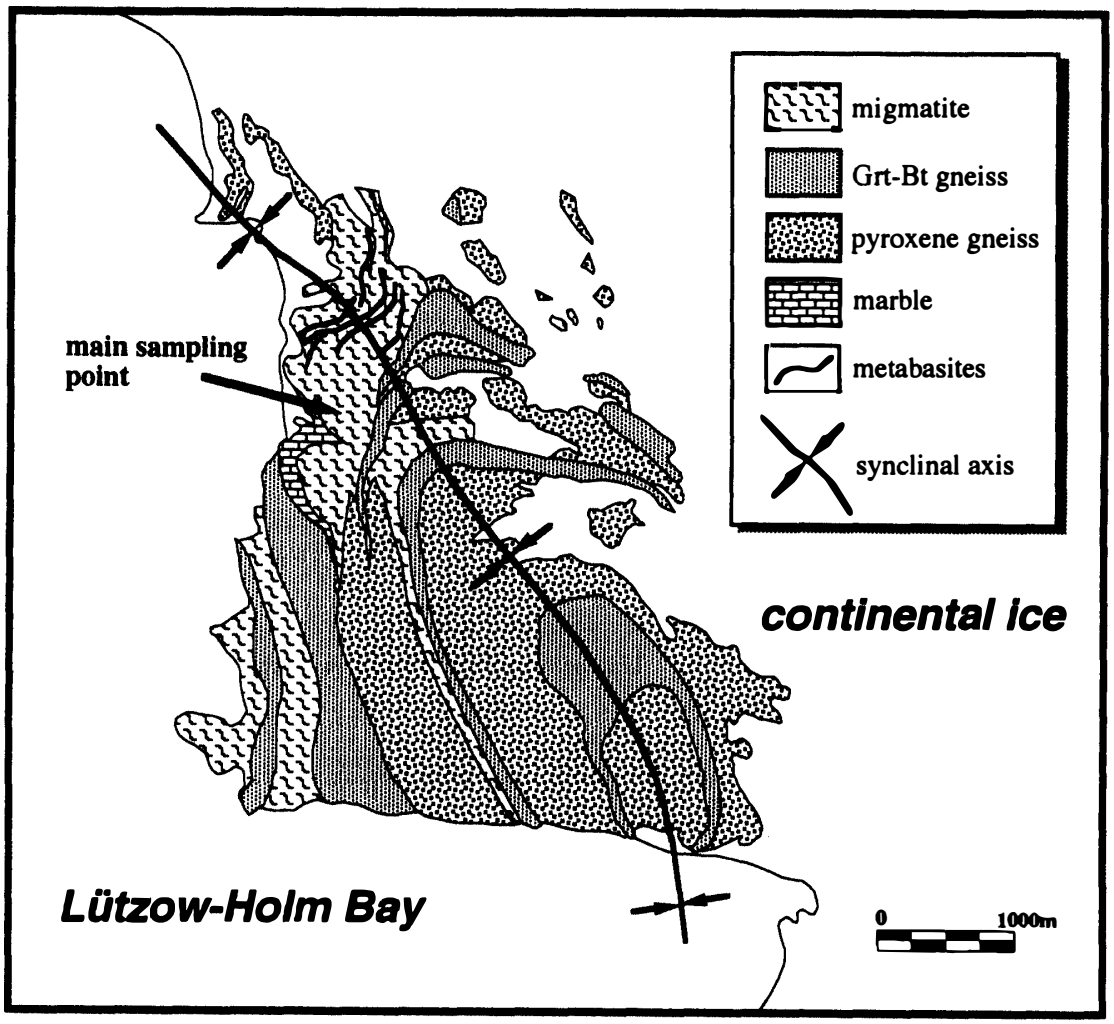

Fig. 2. Simplified geological map of Breidvågnipa (modified after ISHIKAWA et al., 1977). The main sampling site is also shown.

geologists of the Japanese Antarctic Research Expeditions (JARE), and a 1 : 25000 scale geological map of Breidvågnipa has been published (ISHIKAWA *et al.*, 1977). We (TSUCHIYA, SHIMURA, and FRASER) visited Breidvågnipa as members of JARE-35 in 1993–1994. As described later, various types of migmatites are widely distributed in this area.

The geology of Breidvågnipa has been reported by ISHIKAWA (1976) and ISHIKAWA *et al.* (1977). Metamorphic rocks in this area consist mainly of garnet-biotite gneiss, pyroxene gneiss, and marble (Fig. 2). Subordinate amounts of garnet gneiss, garnet-orthopyroxene-biotite gneiss, hornblende-biotite gneissose granite, garnet-biotite granite, and metabasites also occur. The gneiss sequence is folded by a south-east plunging synform, forming a horseshoe shaped outcrop pattern, convex to the north-west. Garnet-biotite gneiss, garnet-orthopyroxene gneiss, and peraluminous granite (garnet-biotite granite) show migmatitic appearance, best exposed in the north-west part of Breidvågnipa.

3. Field Relationships and Petrography of Migmatite and Peraluminous Granite

Various types of migmatites and peraluminous granites are widely distributed at Breidvågnipa. These migmatites are very heterogeneous, and include structures described as agmatic, diktyonitic, stromatic, surreitic, ophthalmitic, sticrolitihic, schlieren, etc. The heterogeneity of these migmatites can be subdivided into three parts: paleosome, melanosome, and leucosome (Fig. 3). Peraluminous granite also occurs intimately with the migmatite (Fig. 4D, E).

Paleosome is relatively fine-grained and forms brownish colored layers. In many cases, the layer is 5 mm–10 cm wide and rimmed by melanosome (Figs. 3, 4). The typical mineral assemblages are garnet, biotite, plagioclase, quartz, and K-feldspar. Paleosome has a schistosity defined by the orientation and distribution of biotite (Fig. 5A), and is commonly composed of an alternation of biotite rich melanocratic layers and leucocratic felsic layers. Garnet is subhedral to anhedral shaped.

Melanosome is the medium- to coarse-grained melanocratic part of the migmatite (Figs. 3, 4). It mainly consists of garnet, biotite, plagioclase, and quartz. Relatively small amounts of K-feldspar are observed. In some cases orthopyroxene also occurs. Melanosome is rich in ferro-magnesian minerals, such as garnet, biotite, and orthopyroxene. Although the melanosome alternated with the leucosome and paleosome, the schistosity is not clear in thin sections (Fig. 5B). Garnet is subhedral to euhedral and encloses small crystals of biotite, plagioclase, and quartz. Melanosome occurs rimming leucosome, and in many cases the width of melanosome increases proportionately with that of the adjacent leucosome (Fig. 3).

Leucosome is the medium- to coarse-grained leucocratic part of the migmatite (Figs. 3, 4). It occurs as layers, dikes, pools, and irregular shapes, and in some cases as segregates in boudin necks (Figs. 3, 4A). Leucosome has no foliation and shows granitic texture (Fig. 5C). It is mainly composed of K-feldspar, plagioclase, and quartz. Distinctively, it is richer in K-feldspar than other parts of the migmatite. Leucosome also contains euhedral to subhedral biotite, euhedral garnet, and/or orthopyroxene. The size of the orthopyroxenes reach as large as 4 cm. Orthopyroxene appears euhedral in outcrops (Fig. 4B), but is rimmed by biotite+quartz intergrowth, and therefore it shows irregular shape

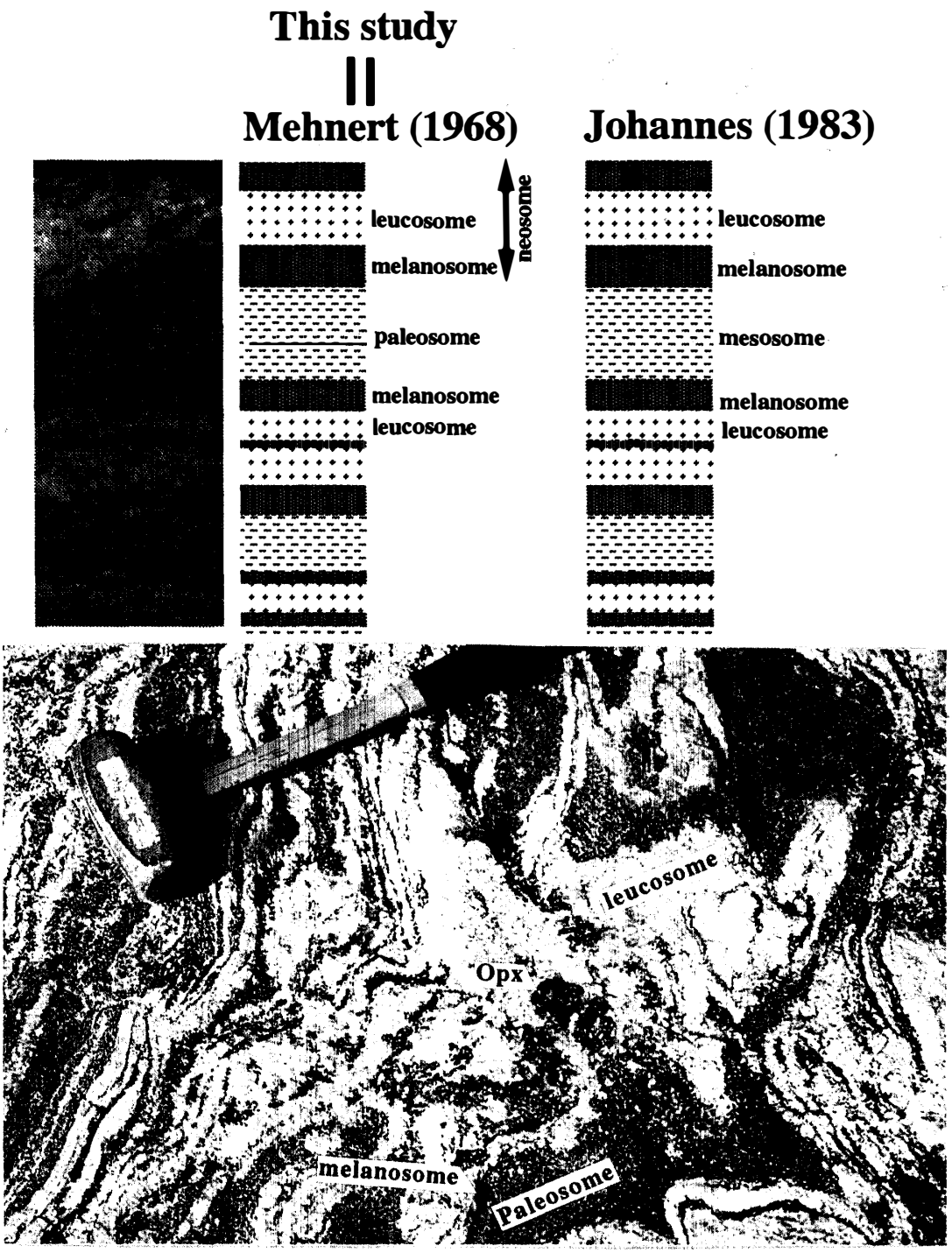

Fig. 3. Migmatite terminology of MEHNERT *(1968),* JOHANNES *(1983), and this paper. Melanosome occurs between leucosome and paleosome. The width of a leucosome is proportional to that of the next melanosome.*

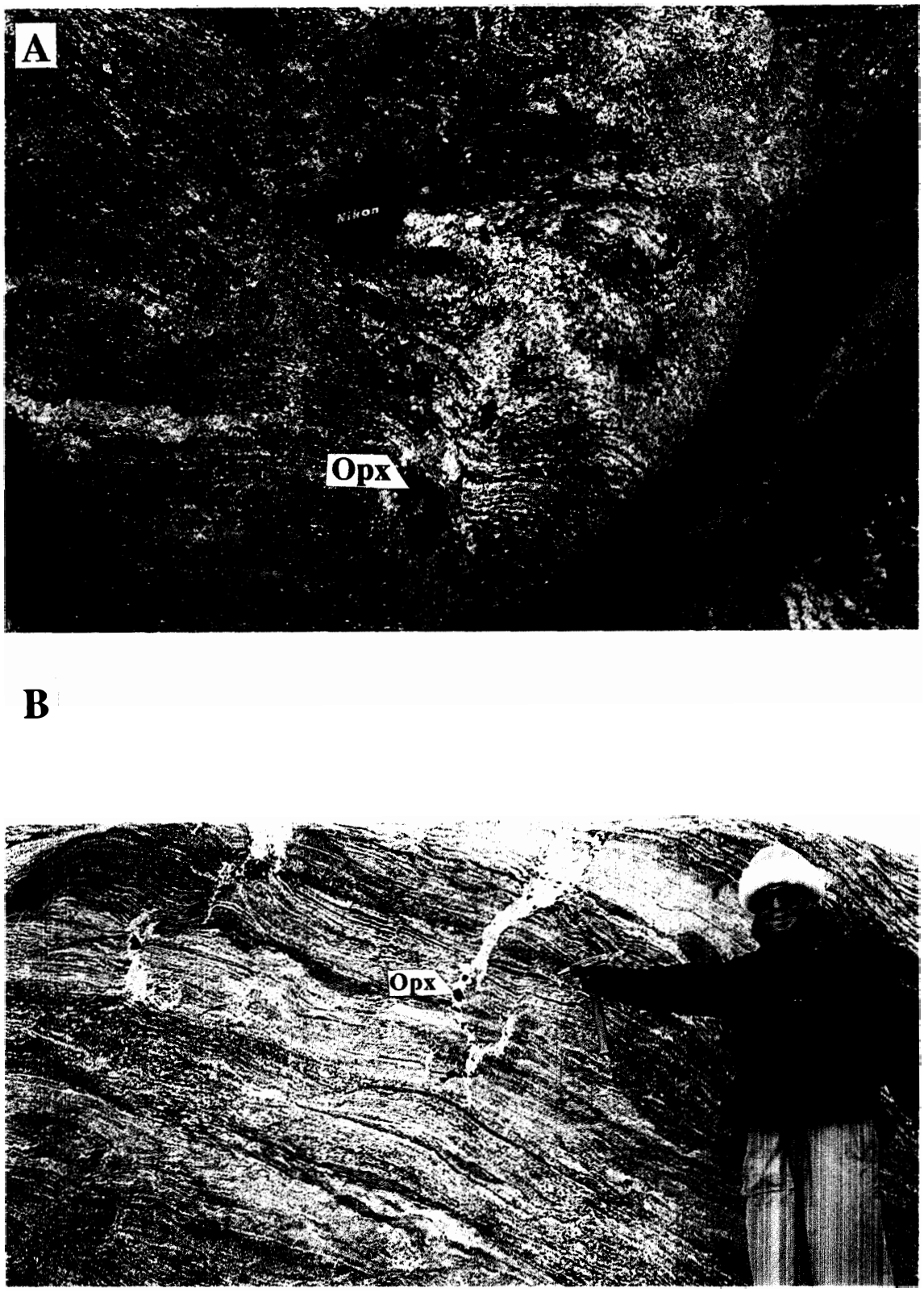

Fig. 4. Field occurrences of migmatite and peraluminous granite at Breidvågnipa. (A) Note the occurrence of a large crystal of orthopyroxene with leucosome cross-cutting the stromatic migmatite at the boudin neck. (B) Leucocratic dikes with euhedral orthopyroxene cut the stromatic migmatite and show stictolithic structure.

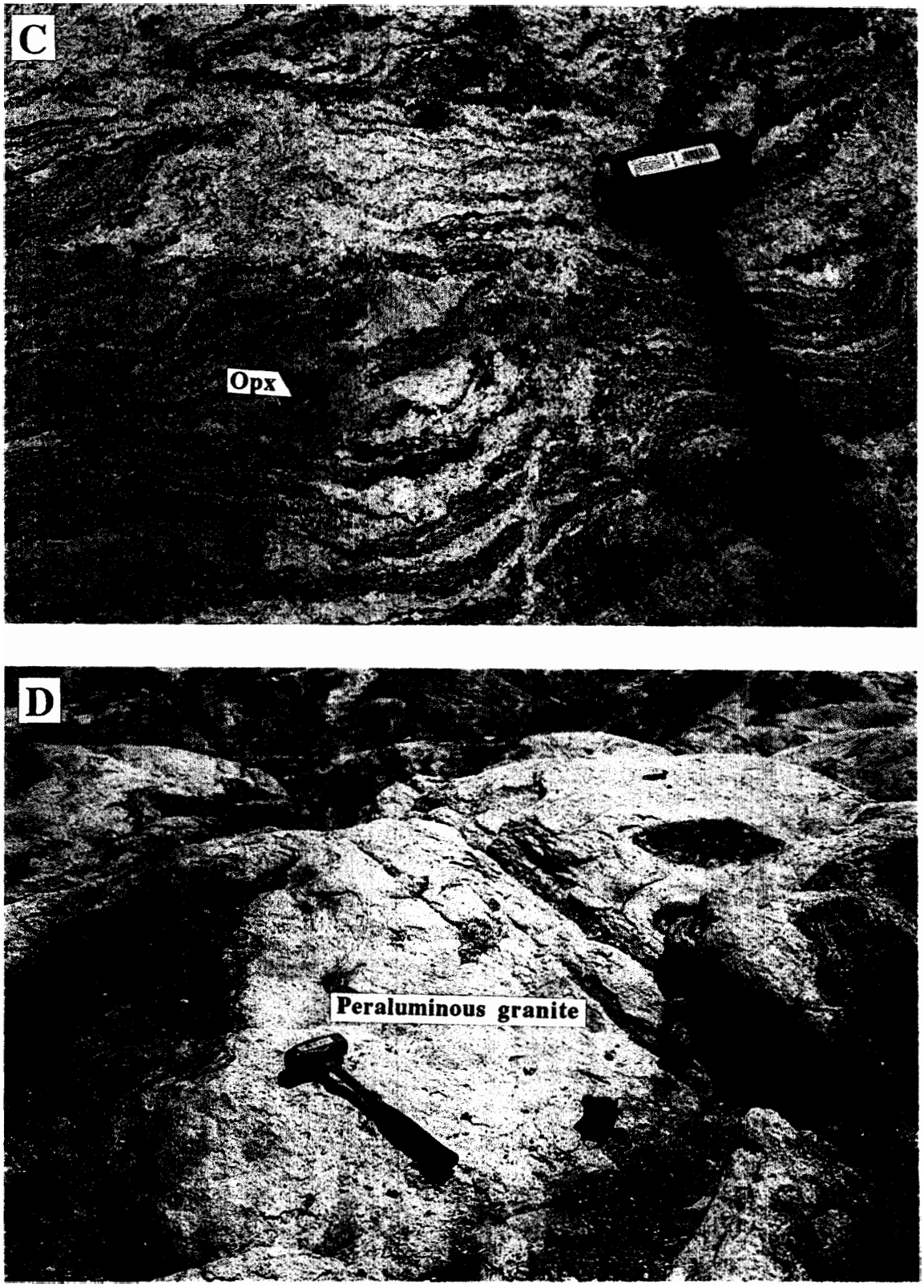

The person for scale is Dr. FRASER. (C) Occurrence of stromatic or schlieren migmatite. (D) Pool-like occurrence of peraluminous granite. (E) A dike of peraluminous granite. Note the irregular shape of the intrusive boundary.

Fig. 4. Continued.

in thin section. Perthite and antiperthite are common in feldspars.

The peraluminous granite occurs as dikes (3 cm–1 m wide) or irregular shaped pools (50 cm–5 m in diameter) (Fig. 4D, E). It is mainly garnet-bearing leucocratic granite and the assemblages are garnet, biotite, plagioclase, K-feldspar, and quartz. Euhedral garnet (1 mm–2 cm in diameter) is common. Small amounts of Garnet-absent biotite granite are also present. The boundaries between these granites and leucosomes are intergradational.

The important features of the relationships in each part of the migmatite and the peraluminous granite in this area are: (1) melanosome occurs between leucosome and paleosome, (2) the volume of leucosome is proportional to that of melanosome, (3) leucosome shows granitic texture and contains euhedral garnet and/or orthopyroxene, and (4) leucosome grades into peraluminous granite.

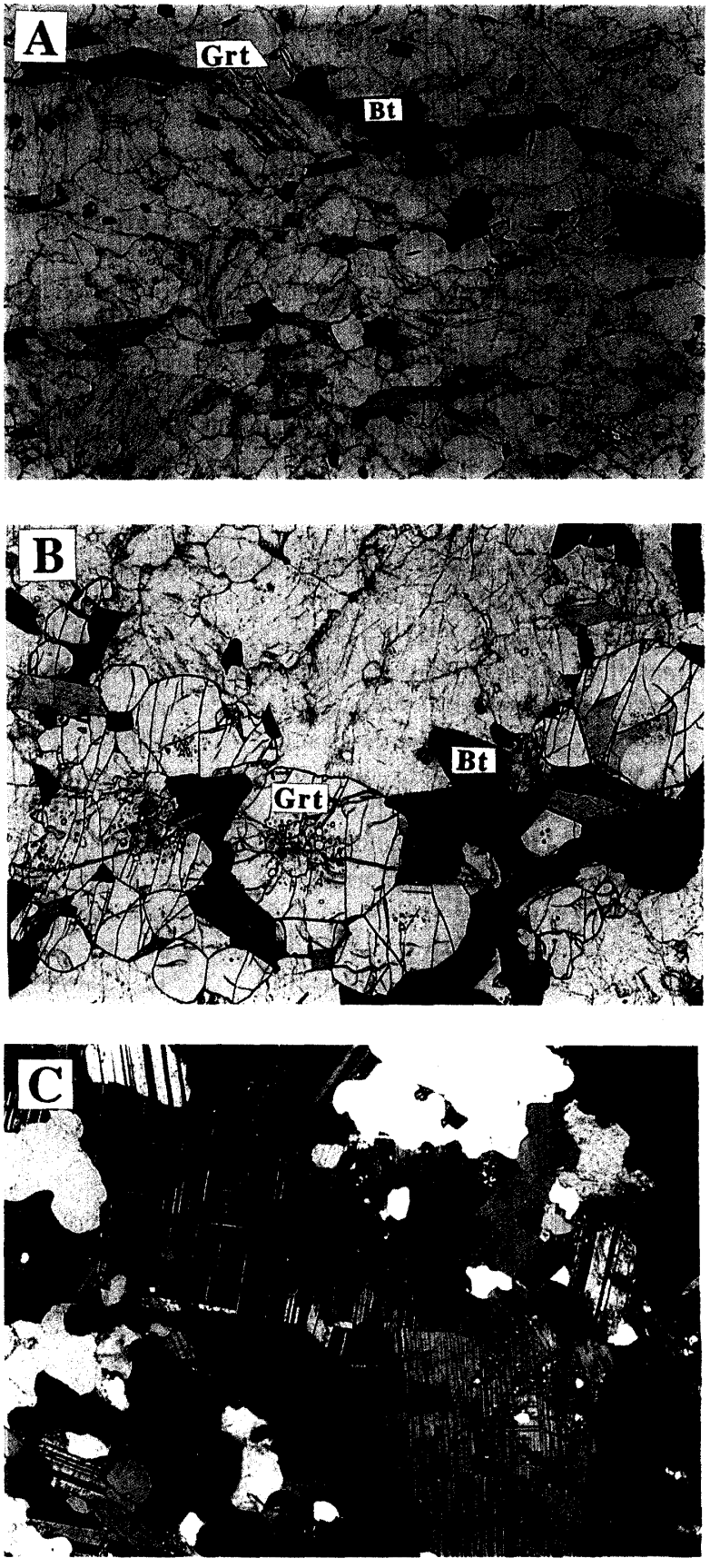

Fig. 5. Photomicrographs of the migmatites. Base of photos = 4.5 mm. (A) Paleosome has schistosity, and the typical mineral assemblage is Grt-Bt-Pl-Qtz. Plane polarized light. (B) melanosome is rich in ferro-magnesian minerals, such as Grt or Opx. Plane polarized light. (C) Leucosome has no foliation and shows granitic texture, and is rich in felsic minerals. Crossed polars.

4. Samples and Analytical Methods

All samples were collected by the authors during JARE-35 (1993-94). Almost all analyzed samples were collected around the north west side of Breidvågnipa (Fig. 2). Granites were sampled from the centers of dikes or pools. Migmatites were separated into paleosome, melanosome, and leucosome by rock-cutter and by hand-picking in the laboratory. Migmatite samples for Rb-Sr measurement (Fig. 13) were separated from a 30 cm-sized sample.

Major element and trace element analysis of whole rocks was carried out by the X-ray fluorescence analyzer (Rigaku IKF-3064) at the Department of Geology, Faculty of Science, Niigata University. Analytical methods for major elements are after NAKAGAWA and KOMATSU (1983), and for trace elements are after TAMURA *et al.* (1989) and KAWANO *et al.* (1992). FeO was determined by the $KMnO_4$ titration method.

Isotope compositions were determined using the mass spectrometer (MAT-261) at the Graduate School of Science and Technology, Niigata University. All of the Rb and Sr concentrations for dating were measured by the isotope dilution method. The "Krough-type" vessels and jackets (KROUGH, 1973) were employed to dissolve the samples. The analytical procedures have been discussed by KAGAMI *et al.* (1987, 1989). $^{87}Sr/^{86}Sr$ ratios were normalized to $^{86}Sr/^{88}Sr=0.1194$. Rb-Sr isochron ages were calculated using the equation of YORK (1966), the ^{87}Rb decay constant $\lambda=1.42\times10^{-11}$/y, and the calculation procedure of KAWANO (1994). The $^{87}Sr/^{86}Sr$ ratio for NBS987 was measured three times during this study, with a mean value of 0.710220 ± 0.000008 (2σ).

Mineral compositions were analyzed by wavelength dispersive X-ray spectroscopy (JEOL JXA-8600MX) at the Graduate School of Science and Technology, Niigata University. Operating conditions were generally 15 kV accelerating voltage, 13 nA sample current, and 1 μm beam diameter. The counting times were 10 s on the peak and 5 s on the background. To analyze trace elements, such as Rb, Ba, F, and Cl, these conditions were changed to 15 kV, 13-60 nA, 5 μm, and 10-30 s on the peak. Three-channel spectrometers were used simultaneously. Na, K, Rb or F were analyzed first to minimize losses. The ZAF correction procedures were used and the analyzed data were transmitted to a personal computer by the system of SHIMURA (1995).

5. Whole Rock Chemical Composition of Migmatite and Granite

Granites of Breidvågnipa are garnet-biotite granite or biotite granite. As a reflection of this mineral assemblage, these granites are slightly peraluminous in composition, having an aluminium saturation index (ASI, mol $Al_2O_3/(CaO+Na_2O+K_2O)$) of 1.02 to 1.11 (Table 1, Figs. 6, 7).

CHAPPELL and WHITE (1974) and WHITE and CHAPPELL (1977) distinguished between S- and I-type granites on the basis of the field occurrences, mineral assemblages, and chemical composition. They compiled the whole rock chemical composition of granites of the Lachlan Fold Belt (LFB) and proposed a boundary between S- and I-type defined by ASI = 1.1. Many subsequent workers have used the ASI value of 1.1 as a strict boundary between S- and I-type granites. Under this criterion the granites from Breidvågnipa are predominantly I-types, but straddle the boundary of S-types. However

Table. 1. Bulk chemical compositions of migmatites and peraluminous granites of Breidvågnipa.

Sample	BVN01	BVN02l	BVN03l	BVN03m	BVN05l	BVN05m	BVN16	BVN32	BVN34	BVN35	BVN36	BVN38	BVN39	BVN40
type	melano	melano	leuco	paleo	leuco	paleo	melano	granite	granite	granite	granite	granite	granite	granite
SiO2	70.821	69.096	70.818	71.833	68.294	68.515	70.372	66.893	74.372	73.275	71.437	73.079	70.985	72.832
TiO2	0.755	0.670	0.381	0.481	0.125	0.611	0.334	0.181	0.020	0.134	0.148	0.186	0.223	0.162
Al2O3	13.897	16.141	15.119	14.121	17.433	14.747	15.157	18.838	14.807	14.822	16.081	15.934	16.182	15.271
Fe2O3	0.584	0.891	0.000	0.451	0.000	0.933	0.479	0.000	0.000	0.000	0.000	0.000	0.083	0.000
FeO	3.391	2.636	1.844	1.638	1.450	3.271	2.172	0.628	0.074	0.374	0.539	0.627	1.671	0.925
MnO	0.070	0.075	0.032	0.033	0.046	0.059	0.059	0.000	0.012	0.005	0.004	0.004	0.030	0.000
MgO	1.241	0.934	0.654	0.695	0.286	1.102	0.656	0.366	0.083	0.263	0.317	0.423	0.731	0.343
CaO	3.151	2.454	2.411	2.122	1.752	2.080	2.301	2.156	2.092	1.450	2.005	1.668	2.214	1.682
Na2O	3.296	4.644	3.122	2.572	4.259	3.752	3.083	4.111	4.090	3.067	3.568	3.446	3.660	3.316
K2O	1.958	1.752	4.950	5.266	5.961	3.896	4.805	6.300	3.636	5.855	5.081	5.242	4.382	5.413
P2O5	0.281	0.131	0.231	0.212	0.038	0.230	0.255	0.057	0.043	0.038	0.040	0.057	0.125	0.032
TOTAL	99.163	99.292	99.331	99.211	99.605	98.964	99.417	99.473	99.185	99.245	99.180	100.610	100.160	99.943
Cr	0	0	0	0	0	0	0	0	0	0	0	0	0	0
Ni	15	14	17	16	17	13	7	2	0	4	4	8	9	16
Rb	82	146	165	188	173	132	115	146	85	141	122	130	139	132
Sr	438	354	784	672	243	180	206	967	749	791	827	689	667	664
V	458	391	399	432	247	37	47	72	42	70	55	40	44	59
Y	14	0	24	10	35	45	57	1	0	0	0	0	8	0
Zr	239	140	132	144	62	237	198	150	110	68	168	237	211	253
Ba	381	411	2388	2159	886	639	761	2057	1170	1996	1702	1695	1344	1521
Nb	7	5.1	8.4	7.5	6.9	12	11	2.3	1.4	1.6	1.4	1.1	2.7	2.3
ASI	1.047	1.153	1.016	1.024	1.047	1.041	1.049	1.076	1.024	1.057	1.071	1.108	1.094	1.063
X Mg	0.361	0.326	0.387	0.377	0.260	0.323	0.310	0.509	0.666	0.556	0.512	0.546	0.428	0.398

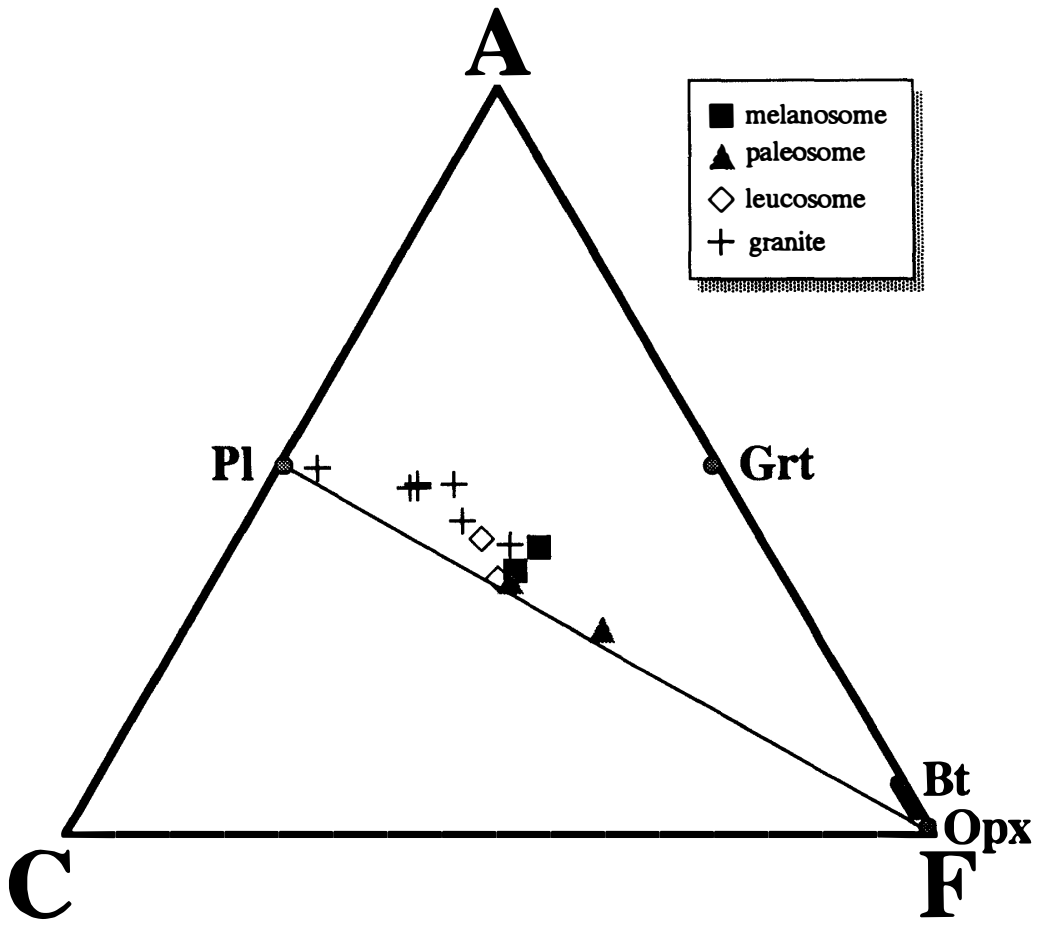

Fig. 6. Bulk chemical compositions of migmatites and peraluminous granites of the study area on ACF ($A = Al_2O_3$-Na_2O-K_2O, $C = CaO$, $F = FeO + MgO$ in molar ratio) diagram.

we believe that an ASI of 1.1 cannot be used in such a strict sense to distinguish S- and I-type granites because the ASI reflects both original rock composition (*e.g.* MONTEL and VIELZEUF, 1997) and the degree of differentiation (CAWTHORN and BROWN, 1976). Note that CHAPPELL and WHITE (1992) also described some overlap between ASI of S- and I-types on the basis of newly analyzed data from the LFB, where ASI values of S- and I-type rocks are 1.01–1.99 and 0.69–1.10 respectively.

The initial $^{87}Sr/^{86}Sr$ ratio (Sr_I) of the granites of Breidvågnipa ranges from 0.7092 to 0.7109 (Table 1, Fig. 7). Many authors have proposed a boundary between the S- and I-type on the basis of Sr_I (*e.g.* CHAPPELL and WHITE, 1974; MURATA, 1984; WHITE *et al.*, 1986; CHAPPELL and WHITE, 1992), but this division is also equivocal. Since the original rock of each area has characteristic Sr_I, the magma reflects the isotopic composition. Therefore the Sr_I of granitoids show distinctive ratios in each area (Fig. 7).

At Breidvågnipa the chemical composition of leucosome is very similar to that of peraluminous granite (Table 1, Figs. 6, 8). These are rich in LIL or incompatible elements compared with paleosome (Fig. 8), whereas melanosome shows depleted composition.

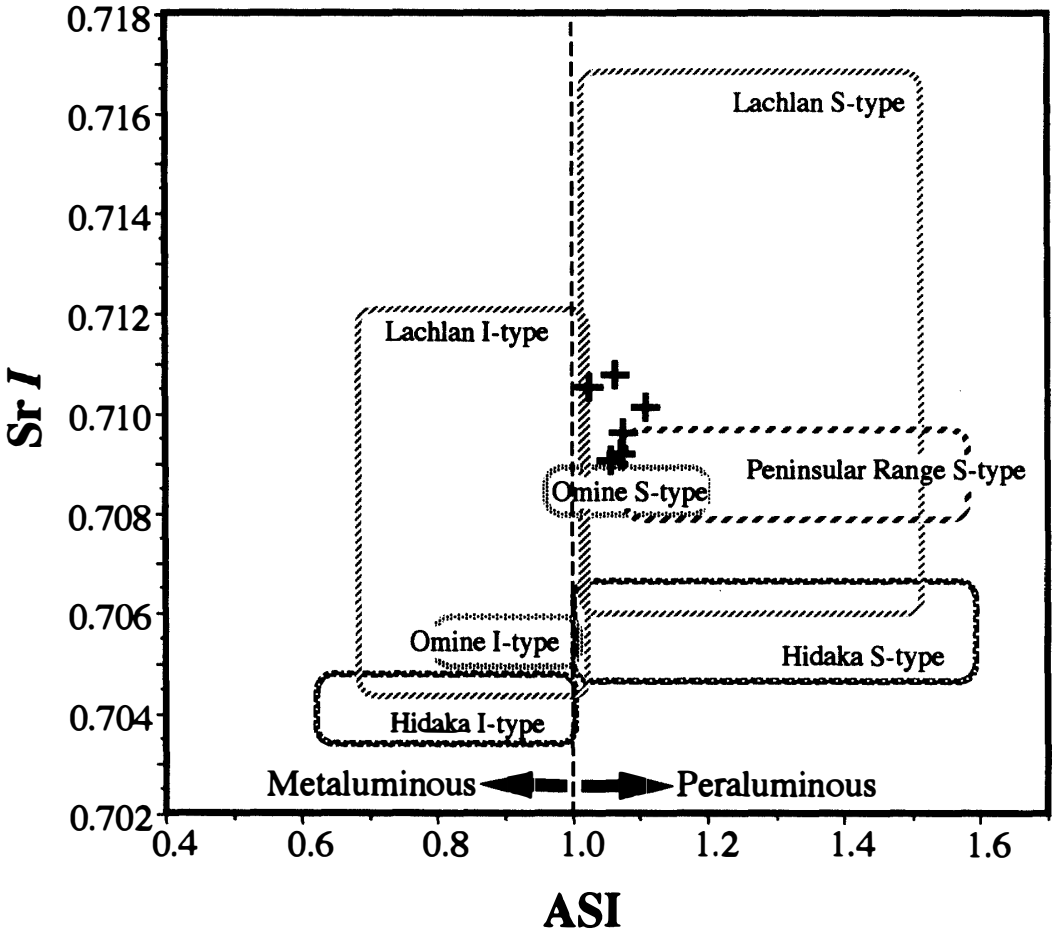

Fig. 7. Aluminium saturation index (ASI)-initial $^{87}Sr/^{86}Sr$ ratio (SrI) values for peraluminous granitoids of Breidvågnipa (cross). Compositional ranges of S- and I-type granitoids are also shown. Data from: CHAPPELL and WHITE (1992), MURATA (1984), TODD and SHAW (1985) and SHIMURA (unpublished data).

6. Mineral Composition of Migmatite

Representative chemical compositions of minerals are shown in the appendix.

X_{Mg} values of garnets in the migmatites range from 0.18 to 0.31 in the core. However, the chemical zoning of each garnet is appreciable, showing relatively uniform cores which range <0.03 units. Sometimes the composition decreases rimward by <0.1 units toward adjacent other Fe-Mg minerals (mainly biotite). We think that the differences of composition are due to the bulk composition, and to chemical diffusion in the garnet by high temperature metamorphism. Weak zoning in the rim is thought to be due to diffusion with other Fe-Mg minerals.

Orthopyroxene has slightly aluminous composition (Fig. 9). The X_{Al} is lower than other granulite facies rocks or experimental results (*e.g.* CONARD *et al.*, 1988; OSANAI *et al.*, 1997; MONTEL and VIELZEUF, 1997). However, the orthopyroxene composition is related to the composition of the host rocks (MAEDA *et al.*, 1991); thus, we suggest that the low X_{Al} content in Opx is due to the relatively low ASI of the host bulk rock compositions

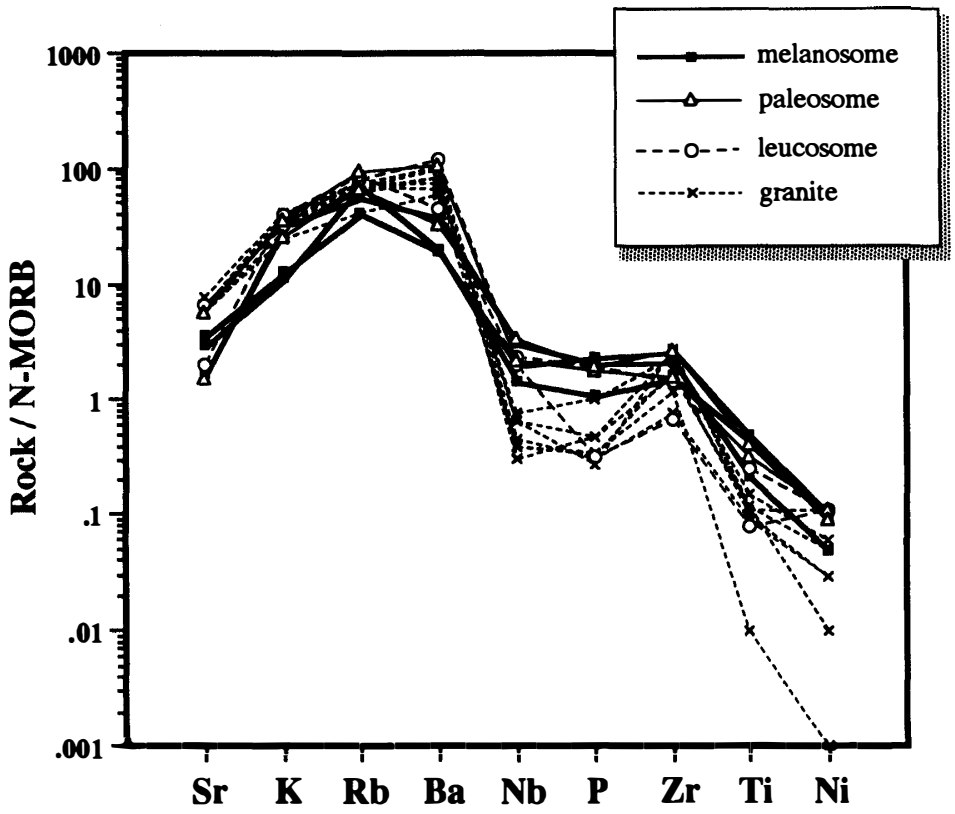

Fig. 8. N-MORB normalized spidergram of migmatite and granite of Breidvågnipa. Note that granite and leucosome are rich in LIL elements compared with paleosome and melanosome.

(ASI = 1.02-1.15) (Table 1).

Biotite is a very common Fe-Mg mineral in pelitic-psammitic metamorphic rocks; the X_{Mg} of biotite is commonly used to estimate metamorphic conditions (THOMPSON, 1976a, b; HOLDAWAY and LEE, 1977). However, especially in granulite facies rocks, other elements such as Al, Ti, Cl, and F are also play important roles in determining the stability of biotite during metamorphism and melting (INDERS and MARTIGNOLE, 1985; PETERSON *et al.*, 1991; KULLERUD, 1995). Biotite compositions of migmatites from Breidvågnipa are shown in Fig. 10. Biotite in the melanosome has higher X_{Mg}, Al^{VI}, Al^{IV} and F, and lower OH, than that of paleosome and leucosome. The main substitution in the X-site is between K and Ba.

Plagioclase and K-feldspar show $An = 20.3$-33.5 and $Or = 63.7$-87.2, respectively. However, many feldspars in the migmatite show perthite and antiperthite, especially in the leucosome (Fig. 5C). These compositions are $An = 5.2$-22.1 for the perthite part in K-feldspar, and $Or = 87.5$-90.5 for the antiperthite in plagioclase.

7. Metamorphism and Melting Reactions

Migmatites at Breidvågnipa contain the aluminosilicate-free assemblage, Grt±Opx+Bt+Pl+Kfs+Qtz. Relatively few published geothermobarometers are applicable to this assemblage in the granulite-facies. Geothermobarometry on this assemblage is compli-

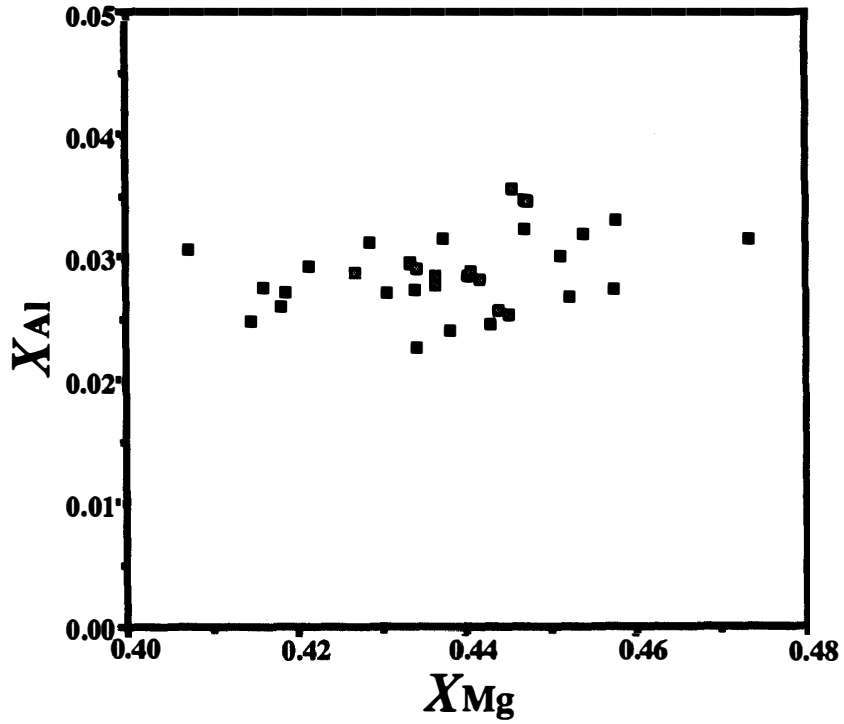

Fig. 9. X_{Al}-X_{Mg} *diagram of orthopyroxene in the migmatite.* $X_{Al}=Al/2$ *and* $X_{Mg}=Mg/(Fe+Mg)$, *on* $O=6$ *per formula unit.*

cated by uncertainties in the activity-composition relationships of biotite, related to Al and Ti content in octahedral sites, and content of Cl, F, Ba, as well as by uncertainties in oxygen fugacity. For this study we have used the following geothermometers: Grt-Bt (INDARES and MATIGNOLE, 1985; DASGUPTA *et al.*, 1991; GESSMAN *et al.*, 1997), Grt-Opx (SEN and BATTACHARYA, 1984; ARANOVICH and KOSYAKOVA, 1984), Opx-Bt (SENGUPTA *et al.*, 1990), and geobarometers: Grt-Opx-Pl (NEWTON and PERKINS, 1982; PERKINS and CHIPERA, 1985).

The calculated results are shown in Fig. 11, and indicate *P-T* conditions for the migmatites at Breidvågnipa of about 0.8 GPa and 870°C. These *P-T* conditions are slightly lower than those estimated for the highest grade rocks in the LHC, at Rundvågshetta, where peak *P-T* conditions reached 1 GPa and ~1000°C (MOTOYOSHI and ISHIKAWA, 1998). The difference in *P-T* conditions between Breidvågnipa and Rundvågshetta gives an apparent geothermal gradient on the order of 20°C/km, assuming that apparent peak *P-T* conditions were reached synchronously in both areas.

One of the important petrographical features of the migmatites at Breidvågnipa is that the leucosome with euhedral garnet or orthopyroxene cuts the biotite-rich paleosome (Fig. 4A). This texture is regarded as a result of the following fluid-absent melting, biotite-breakdown reactions (VIELZEUF and HOLLOWAY, 1988):

$$Bt+Qtz=Opx+Kfs+M \quad (1)$$
$$Bt+Qtz=Grt+Opx+Kfs+M \quad (2)$$
$$Bt+Pl+Qtz=Opx+Kfs+M \quad (3)$$

These reactions occur at about 850-900°C and produce peraluminous granitic melt (GREEN, 1976; VIELZEUF and HOLLOWAY, 1988; LE BRETON and THOMPSON, 1988; PATIÑO

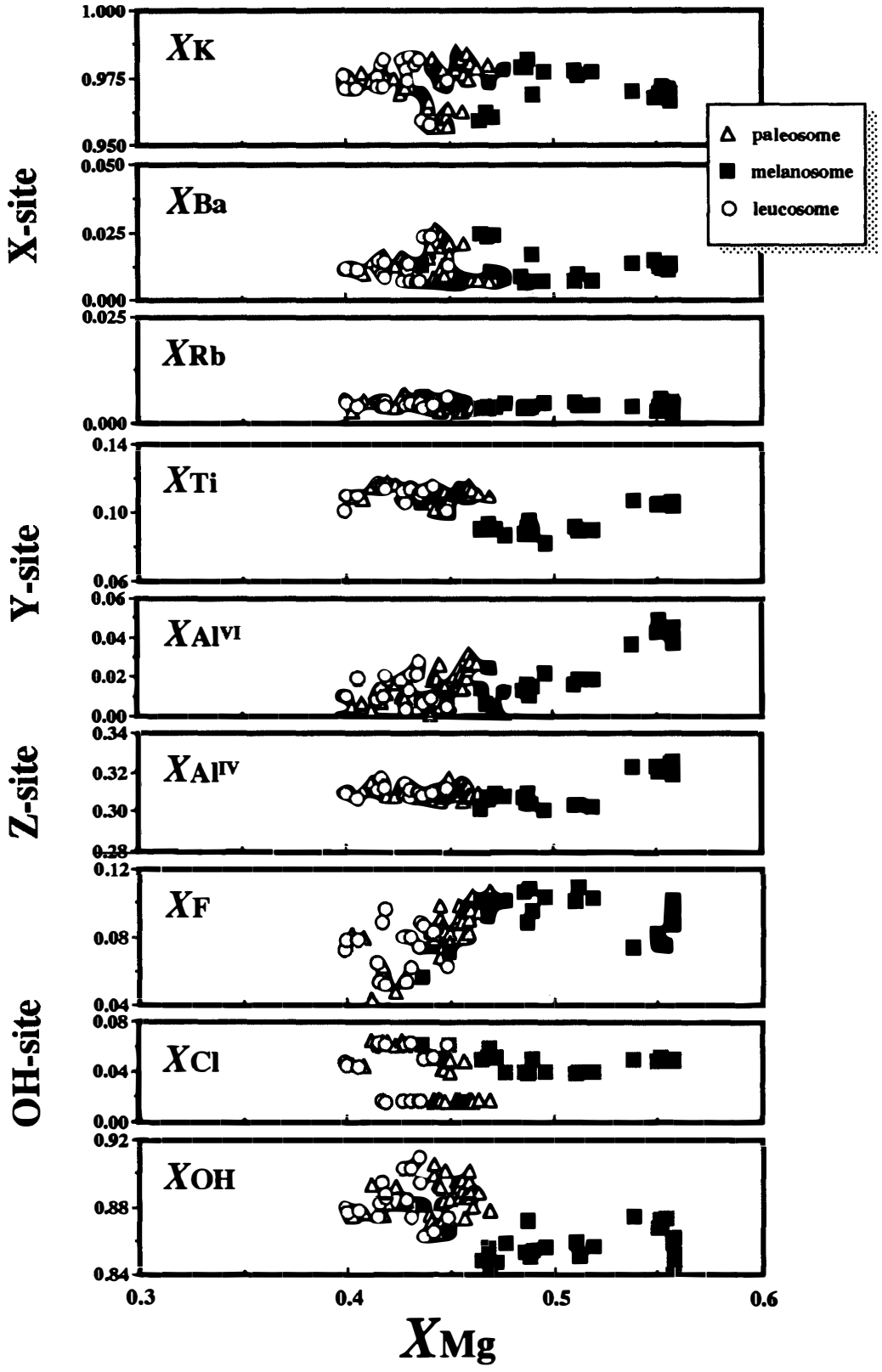

Fig. 10. Chemical composition of biotite in the migmatites. The calculation methods of molecular of each element refer to Table A4 of the appendix.

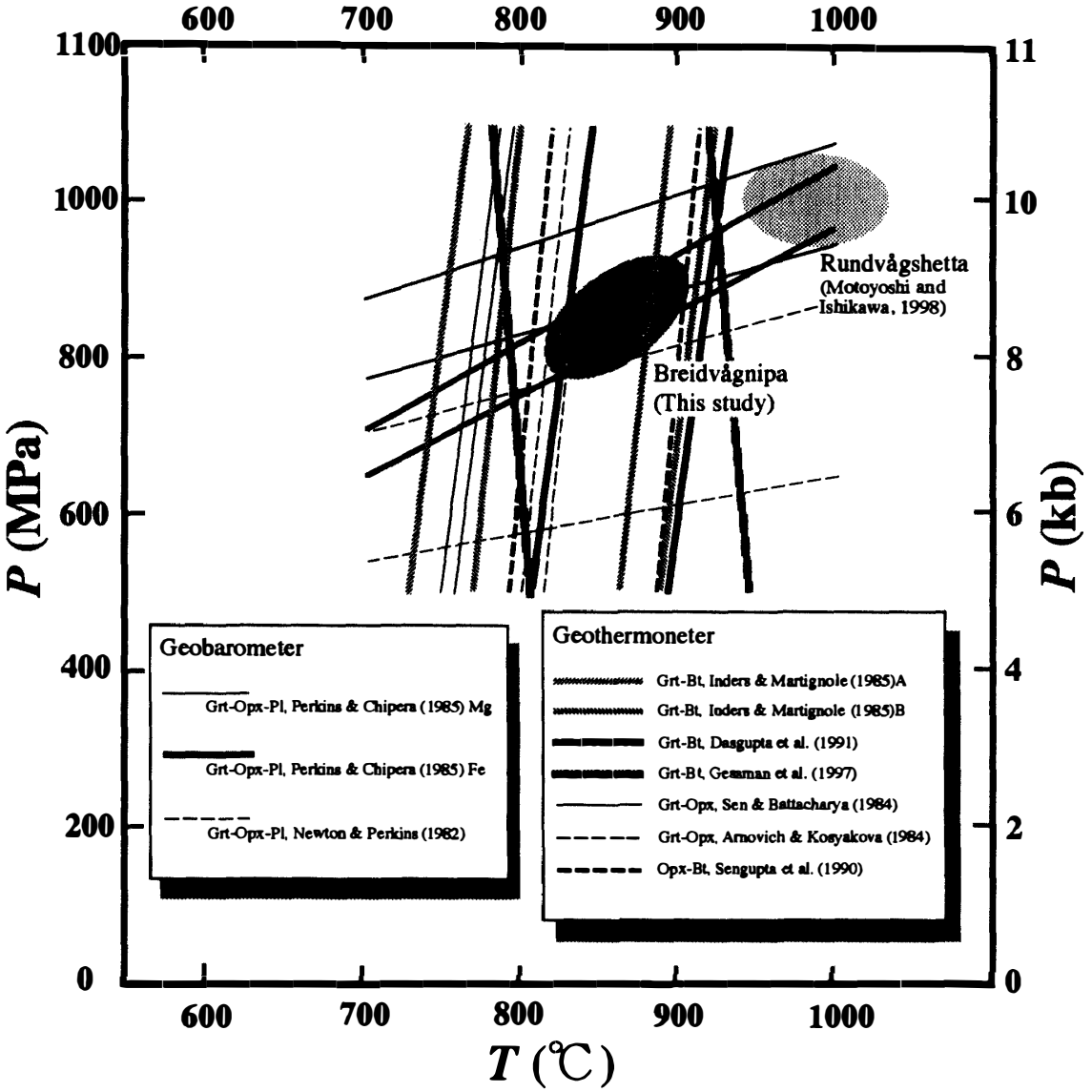

Fig. 11. Calculated results of geothermometers and geobarometers for the migmatite of Breidvågnipa. The peak P-T conditions of Breidvågnipa are thought to be about 800 MPa and 870°C. The highest P-T condition in the LHC (Rundvågshetta, after Motoyoshi *and* Ishikawa, *1998) is also shown.*

Douce and Johnston, 1991; Shimura *et al.*, 1992; Skjerlie *et al.*, 1993; Vielzeuf and Montel, 1994) (Fig. 12).

The biotite-breakdown temperature is a function of several factors, including mineral assemblage, bulk composition (X_{Mg} and ASI), biotite composition (X_{Mg}, F, and Cl), oxygen fugacity, and fluid composition (X_{H_2O}, and X_{CO_2}) (Peterson *et al.*, 1991; Hensen and Osanai, 1994; Dooley *et al.*, 1996; Patiño Douce and Beard, 1996; Carrington and Harley, 1995; Clemens *et al.*, 1997). In general, these studies indicate that the restite phase has higher X_{Mg} , higher X_F (biotite), lower X_{H_2O}, and lower incompatible elements, than the melt phase.

At Breidvågnipa, leucosome is rich in incompatible elements compared with

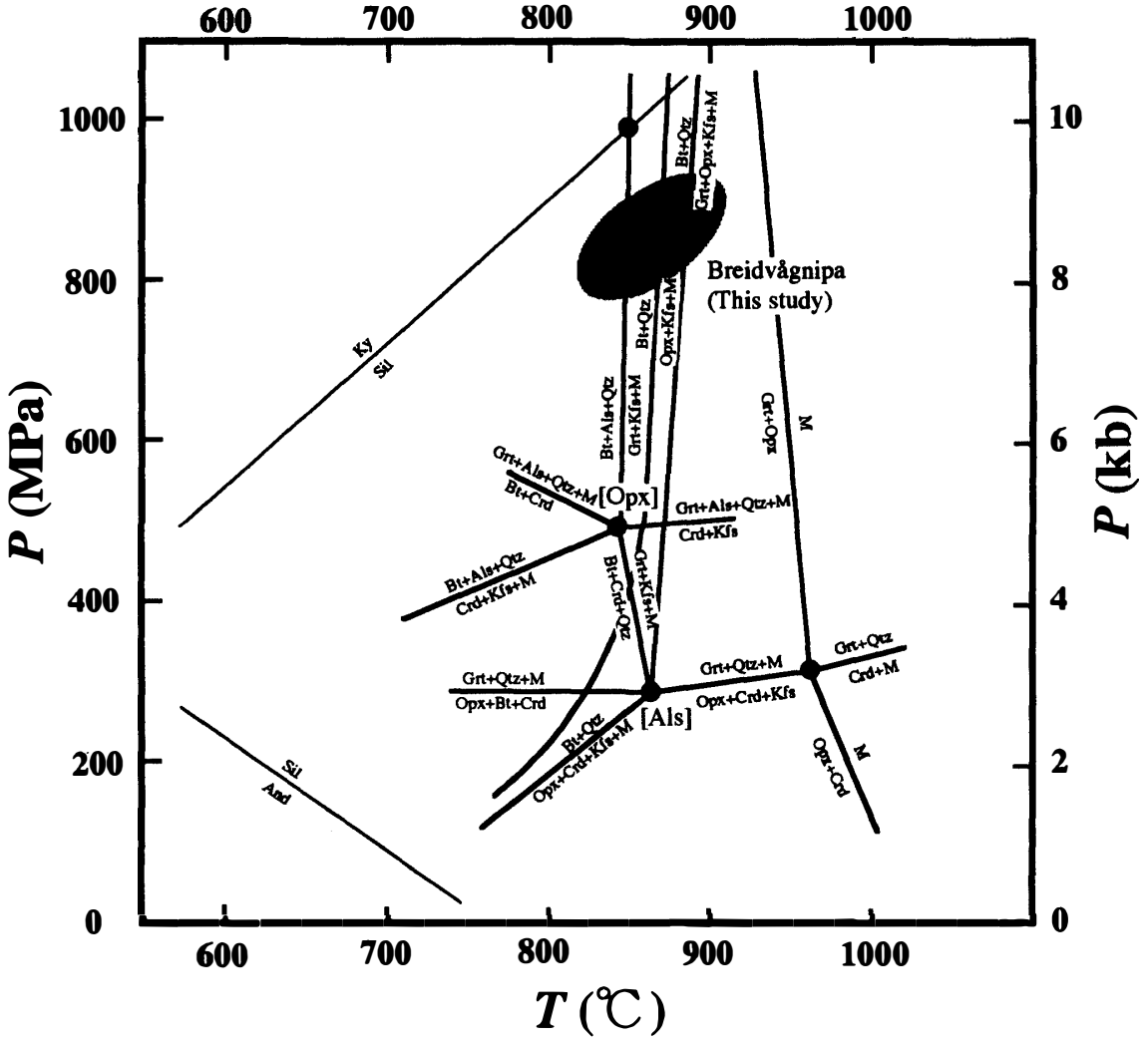

Fig. 12. P-T diagram for fluid-absent partial melting reaction. P-T condition of Breidvågnipa is also shown. Modified from VIELZEUF *and* HOLLOWAY *(1988).*

paleosome (Fig. 8), and melanosome shows depleted composition. Biotites in melanosome are rich in F and poor in OH compared with those of the leucosome (Fig. 10). These features are consistent with paleosome, melanosome, and leucosome and granite representing original rock, restite, and melt, respectively. Consequently, the heterogeneities of the migmatites of this area are thought to be generated by partial melting of pelitic metamorphic rock.

8. Rb-Sr Isochron Age of Migmatite

As described in the previous section, the heterogeneities of the migmatites at Breidvågnipa are thought to have been generated by partial melting during granulite-facies metamorphism of the LHC. Since the parts of the migmatite (paleosome, melanosome, leucosome, and granite), are heated and generated simultaneously, they are expected to have been isotopically homogenized at the time of melting.

Table 2. Rb-Sr analytical data for migmatites and peraluminous granites of Breidvågnipa.

Migmatite

Sample	Rb(ppm)	Sr(ppm)	$^{87}Sr/^{86}Sr$	±(2σ)	$^{87}Rb/^{86}Sr$	Sr*I*
BVN06P	137	286	0.72171	0.000012	1.387	0.71006
BVN06M	231	176	0.74252	0.000014	3.793	0.71068
BVN06L1	41.8	751	0.71284	0.000012	0.161	0.71149
BVN06L2	57	605	0.71344	0.000012	0.439	0.70976
BVN06P2	157	300	0.72188	0.000035	1.517	0.70914
BVN06P3	139	371	0.71887	0.000012	1.087	0.70974
BVN06N1	157	295	0.72215	0.000018	1.541	0.70922
BVN06N2	112	404	0.71680	0.000012	0.804	0.71005
BVN06N3	129	419	0.71751	0.000012	0.892	0.71003

Granite

Sample	Rb(ppm)	Sr(ppm)	$^{87}Sr/^{86}Sr$	±(2σ)	$^{87}Rb/^{86}Sr$	Sr*I*
BVN34	85	749	0.71255	0.000010	0.234	0.71058
BVN32	146	967	0.71336	0.000013	0.437	0.70969
BVN35	141	791	0.71348	0.000013	0.515	0.70916
BVN36	122	827	0.71286	0.000014	0.428	0.70927
BVN38	130	689	0.71483	0.000014	0.548	0.71022
BVN40	132	664	0.71569	0.000014	0.576	0.71085

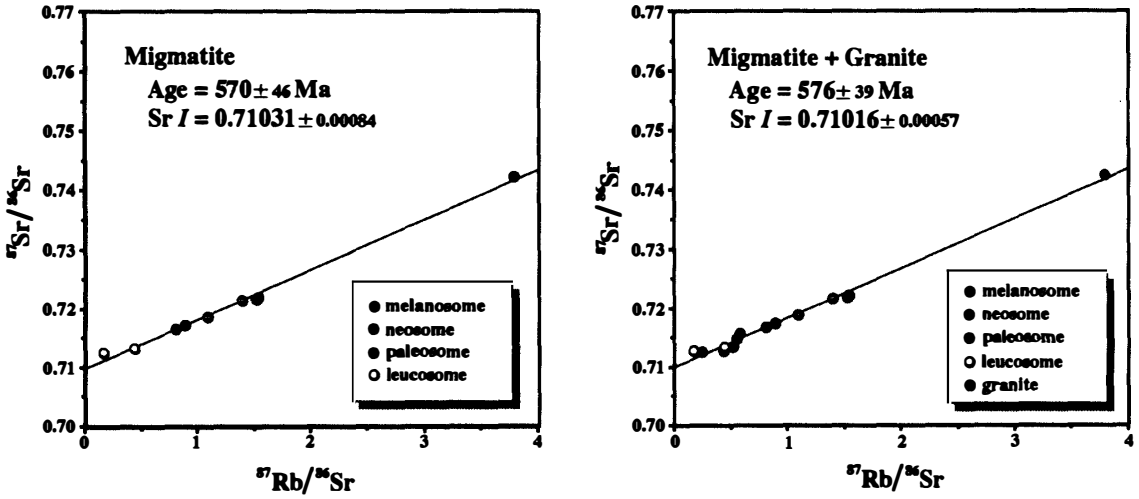

Fig. 13. Rb-Sr isochron diagram of migmatite and peraluminous granite.

Several parts of the migmatite were separated from a 30 cm-sized heterogeneous sample, BVN06. These were subdivided into melanosome, neosome, paleosome, and leucosome. The neosome is a mixture of melanosome and leucosome. Granites were also sampled from the nearby area (Fig. 2).

Rb-Sr results for these separates are shown in Table 2 and Fig. 13. All samples of the migmatite yield an isochron with an age of ~570 Ma. Peraluminous granites also lie almost on this isochron. The errors are relatively large; however, the ages are consistent with Pan-African U-Pb zircon ages from other parts of the LHC (SHIRAISHI *et al.*, 1994).

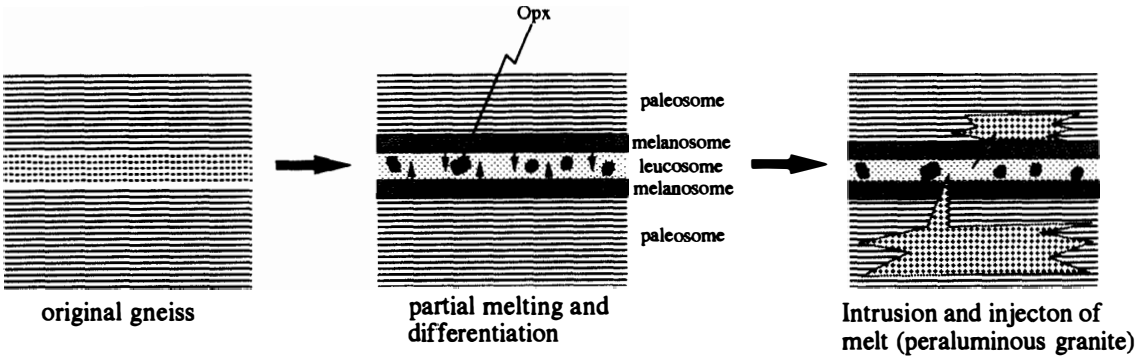

Fig. 14. Schematic picture showing the genesis of the migmatite of Breidvågnipa.

In contrast, MAEGOYA *et al.* (1968) reported whole-rock isochron ages of ~1100 Ma from LHC and Breidvågnipa. We suggest that these ages do not represent the time of metamorphism, as the samples were collected from a very wide area, and are unlikely to have isotopically homogenized even during granulite-facies metamorphism. We calculated the following Bt-Kfs mineral isochron ages from the data of MAEGOYA *et al.* (1968): sample A-01 yields ~452 Ma, and sample A-24 yields ~482 Ma. These ages most likely represent cooling following the granulite-facies metamorphic event, and are consistent with numerous K/Ar and $^{40}Ar/^{39}Ar$ cooling ages reported by FRASER and MCDOUGALL (1995) from throughout the LHC.

9. Conclusions

The evolution of migmatites at Breidvågnipa is summarized in Fig. 14. Biotite break-down reactions occurred at ~870°C, producing peraluminous granitic melt, and resulting in differentiation of the original pelitic gneiss into restite (melanosome) and melt (leucosome). The melt segregated and intruded into the gneiss or migmatite, as dikes and pools of peraluminous granite. Partial melting occurred at ~570 Ma, consistent with previous Pan-African age determinations for high-grade metamorphism in the LHC. The peak *P-T* conditions of metamorphism at Breidvågnipa were ~0.8 GPa and ~870°C, slightly lower grade than conditions reported for Rundvågshetta (MOTOYOSHI and ISHIKAWA, 1998).

Acknowledgments

We wish to thank all members of JARE-35 (1993-94) and the crew of the icebreaker SHIRASE for their support in the fieldwork. Prof. K. SHIRAISHI, Prof. Y. HIROI, Dr. Y. MOTOYOSHI, Prof. Y. TAINOSHO, Dr. Y. OSANAI, and Dr. M. OWADA are thanked for their helpful discussions. Dr. M. YUHARA and Mr. T. HAMAMOTO assisted in the MAS analysis, and Ms. R. SHIMURA helped with the figure drawings. Part of this work was supported by the Grant in Aid for Scientific Research of the Ministry of Education (No. 07740400, T.S. and 07304041, H.K.).

References

ARANOVICH, L.Ya. and KOSYAKOVA, N.A. (1984): Experimental study of cordierite+orthopyroxene+quartz equilibrium in the system FeO-MgO-Al_2O_3-SiO_2. Dokl. Akad. Nauk SSSR, **274**, 399-401.

ASHWORTH, J.R. (1985): Migmatites. Glasgow, Blackie, 301 p.

ATHERTON, M.P. and GRIBBLE, C.D. (1983): Migmatites, Melting and Metamorphism. Nantwich, Shiva Publishing Ltd., 326 p.

CARRINGTON, D.P. and HARLEY, S.L. (1995): Partial melting and phase relations in high-grade metapelites: An experimental petrogenetic grid in the KFMASH system. Contrib. Mineral. Petrol., **120**, 270-291.

CAWTHORN, R.G. and BROWN, P.A. (1976): A model for the formation and crystallization of corundum-normative calc-alkaline magmas through amphibole fractionation. J. Geol., **84**, 467-476.

CHAPPELL, B.W. and WHITE, A.J.R. (1974): Two contrasting granite types. Pac. Geol., **8**, 173-174.

CHAPPELL, B.W. and WHITE, A.J.R. (1992): I- and S-type granites in the Lachlan Fold Belt. Trans. R. Soc. Edinburgh, **83**, 1-26.

CLEMENS, J.D., DROOP, G.T.R. and STEVENS, G. (1997): High-grade metamorphism, dehydration and crustal melting: A reinvestigation based on new experiments in the silica-saturated portion of the system $KAlO_2$-MgO-SiO_2-H_2O-CO_2 at $P \leq 1.5$ GPa. Contrib. Mineral. Petrol., **129**, 308-325.

CONRAD, W.K., NICHOLLS, I.A. and WALL, V.J. (1988): Water-saturated and -undersaturated melting of metaluminous and peraluminous crustal compositions at 10 kb: Evidence for the origin of silicic magmas in the Taupo volcanic zone, New Zealand, and other occurrences. J. Petrol., **29**, 765-803.

DASGUPTA, S., SENGUPTA, P., GUHA, D. and FUKUOKA, M. (1991): A refined garnet-biotite Fe-Mg exchange geothermometer and its application in amphibolites and granulites. Contrib. Mineral. Petrol., **109**, 130-137.

DEER, W.A., HOWIE, R.A. and ZUSSMAN, J. (1992): An Introduction to the Rock-forming Minerals. 2nd ed. Essex, Longman, 696 p.

DOOLEY, D.F. and PATIÑO DOUCE, A.E. (1996): Fluid-absent melting of F-rich phlogopite+rutile+quartz. Am. Mineral., **81**, 202-212.

FRASER, G. and MCDOUGALL, I. (1995): K/Ar and $^{40}Ar/^{39}Ar$ mineral ages across the Lürzow-Holm Complex, East Antarctica. Proc. NIPR Symp. Antarc. Geosci., **8**, 137-159.

FRASER, G., MCDOUGALL, I., ELLIS, D. and WILLIAMS, I.S. (1997): Timing, extent and rate of isothermal decompression following granulite-facies metamorphism at Rundvågshetta, East Antarctica. The 17th Symp. Antarct. Geosci. Program Abstracts. Tokyo, Natl Inst. Polar Res., 30-31.

GESSMAN, C.K., SPIERING, B. and RAITH, M. (1997): Experimental study of the Fe-Mg exchange between garnet and biotite: Constraints on the mixing behavior and analysis of the cation-exchange mechanisms. Am. Mineral., **82**, 1225-1240.

GREEN, T.H. (1976): Experimental generation of cordierite- or garnet-bearing granitic liquids from a pelitic composition. Geology, **4**, 85-88.

HENSEN, B.J. and OSANAI, Y. (1994): Experimental study of dehydration melting of F-biotite in model pelitic compositions. Mineral. Mag., **58A**, 410-411.

HIROI, Y., SHIRAISHI, K. and MOTOYOSHI, Y. (1991): Late Proterozoic paired metamorphic complexes in East Antarctica, with special reference to the tectonic significance of ultramafic rocks. Geological Evolution of Antarctica, ed. by M.R.A. THOMSON *et al.* Cambridge, Cambridge University Press, 83-87.

HOLDAWAY, M.J. and LEE, S.M. (1977): Fe-Mg cordierite stability in high-grade pelitic rocks based on experimental, theoretical, and natural observations. Contrib. Mineral. Petrol., **63**, 175-198.

INDARES, A. and MARTINGNOLE, J. (1985): Biotite-garnet geothermometry in the granulite facies: the influence of Ti and Al in biotite. Am. Mineral., **70**, 272-278.

ISHIKAWA, T. (1976): Superimposed folding of the Precambrian metamorphic rocks of the Lützow-

Holm Bay region, East Antarctica. Mem. Natl Inst. Polar Res., Ser. C, **9**, 1-41.

ISHIKAWA, T., YANAI, K., MATSUMOTO, Y., KIZAKI, K., KOJIMA, S., TATSUMI, T., KIKUCHI, T. and YOSHIDA, M. (1977): Geological map of Skarvsnes. Antarctic Geological Map Series, Sheet 6 and 7 (with explanatory 10 p.). Tokyo, Natl Inst. Polor Res.

JOHANNES, W. (1983): On the origin of layerd migmatites. Migmatites, Malting and Metamorphism, ed. by M.P. ATHERTON and C.D. GRIBBLE. Cheshire, Shiva, 234-248.

JOHANNES, W., HOLTZ, F. and MÖLLER, P. (1995): REE distribution in some layered migmatites: Constraints on their petrogenesis. Lithos, **35**, 139-152.

KAGAMI, H., IWATA, M., SANNO, S. and HOMMA, H. (1987): Sr and Nd isotopic compositions and Rb, Sr, Sm and Nd concentrations of standard samples. Tech. Rep. ISEI Okayama Univ., Ser. **B4**, 16 p.

KAGAMI, H., YOSOSE, H. and HOMMA, H. (1989): $^{87}Sr/^{86}Sr$ and $^{143}Nd/^{144}Nd$ ratios of GSJ rock reference samples; JB-1a, JA-1 and JG-1a. Geochem. J., **23**, 209-214.

KAWANO, Y. (1994): Calculation program for isochron ages of Rb-Sr and Sm-Nd systems, using personal computer. Geoinformatics, **5**, 1-53.

KAWANO, Y., WATANABE, N., YAMAMOTO, K. and SHUTO, K. (1992): Quantitative analysis of Ba, Co, and V in silicate rocks by X-ray fluorescence method. Contrib. Dept. Geol. Mineral. Niigata Univ., **7**, 111-115.

KRETZ, R. (1983): Symbols for rock-forming minerals. Am. Mineral., **68**, 277-279.

KROUGH, T.E. (1973): A low-contamination method for hydrothermal decomposition of zircon and extraction of U and Pb for isotopic age determinations. Geochim. Cosmochim. Acta, **37**, 485-494.

KULLERUD, K. (1995): Chlorine, titanium and barium-rich biotites: Factors controlling biotite composition and the implications for garnet-biotite geothermometry. Contrib. Mineral. Petrol., **120**, 42-59.

LE BRETON, N. and THOMPSON, A.B. (1988): Fluid-absent (dehydration) melting of biotite in metapelites in the early stages of crustal anatexis. Contrib. Mineral. Petrol., **99**, 226-237.

MAEDA, J., SHIMURA, T., ARITA, K., OSANAI, Y., MURATA, M., BAMBA, M. and SUETAKE, S. (1991): Chemical features of orthopyroxene in peraluminous igneous rocks. Am. Mineral., **76**, 1676-1684.

MAEGOYA, T., NOHDA, S. and ICHIKAZU, H. (1968): Rb-Sr dating of the gneissic rocks from the east cost of Lützow-Holm Bay, Antarctica. Mem. Fac. Sci., Kyoto Univ., Ser. Geol. Mineral., **35**, 131-138.

MEHNERT, K.R. (1968): Migmatites and the Origin of Granitic Rocks. Amsterdam, Elsevier, 393 p.

MIYASHIRO, A. (1994): Metamorphic Petrology. New York, Oxford Univ. Press, 404 p.

MONTEL, J.M. and VIELZEUF, J. (1997): Partial melting of metagreywackes, Part II. Compositions of minerals and melts. Contrib. Mineral. Petrol., **128**, 176-196.

MOTOYOSHI, Y. and ISHIKAWA, M. (1998): Metamorphic and structural evolution of granulites from Rundvågshetta, Lützow-Holm Bay, East Antarctica. The Antarctic Region: Geological Evolution and Processes, ed. by C.A. RICCI. Siena, Terra Antarctic Publ., 65-72.

MOTOYOSHI, Y., MATSUBARA, S. and MATSUEDA, H. (1989): *P-T* evolution of the granulite-facies rocks of the Lützow-Holm Bay region, East Antarctica. Evolution of Metamorphic Belts, ed. by J.S. DALY *et al*. Oxford, Blackwell, 325-329 (Geol. Soc. Spec. Publ. **43**).

MURATA, M. (1984): Petrology of Miocene I-type and S-type granitic rocks in the Ohmine district, central Kii peninsula. J. Jpn. Assoc. Mineral. Petrol. Econ. Geol., **79**, 351-369.

NAKAGAWA, M. and KOMATSU, M. (1983): Bulk rock analysis using automatic X-ray fluorescence analyzer. Petrological Studies of Deep Crust and Upper Mantle Rocks in Island-arc; "Report of research project, grand in aid for scientific research 1982", ed. by M. KOMATSU. Niigata, Niigata Univ., 4-10.

NEWTON, R.C. and PERKINS, III D. (1982): Thermodynamic calibration of geobarometers based on assemblages garnet-plagioclase-orthopyroxene (clinopyroxene)-quartz. Am. Mineral., **67**, 203-222.

OSANAI, Y., OWADA, M., SHIMURA, T., KAWASAKI, T. and HENSEN, B.J. (1997): Crustal anatexis and related acidic magma genesis in the Hidaka metamorphic belt, Hokkaido, northern Japan. Mem. Geol. Soc. Jpn., **47**, 29-42.

PATIÑO DOUCE, A.E. and BEARD, J. (1996): Effects of P, $f(O_2)$ and Mg/Fe ratio on dehydration melting of model metagreywackes. J. Petrol., **37**, 999-1024.

PATIÑO DOUCE, A.E. and JOHNSTON, A.D. (1991): Phase equilibria and melt productivity in the pelitic system: Implications for the origin of peraluminous granitoids and aluminous granulites. Contrib. Mineral. Petrol., **107**, 202-218.

PERKINS, III D. and CHIPERA, S.J. (1985): Garnet-orthopyroxene-plagioclase-quartz barometry: refinement and application to the English River subprovince and the Minnesota River valley. Contrib. Mineral. Petrol., **89**, 69-80.

PETERSON, J.W., CHACKO, T. and KUEHNER, S.M. (1991): The effects of fluorine on the vapor-absent melting of phlogopite+quartz: Implications for deep-crustal processes. Am. Mineral., **76**, 470-476.

SEDERHORM, J.J. (1907): On granite and gneiss. Bull. Comm. Geol. Finl., **23**, 1-110.

SENGUPTA, P., DASGUPTA, S., BHATTACHARYA, P.K. and MUKHERJEE, M. (1990): An orthopyroxene-biotite geothermometer and its application in crustal granulites and mantle-derived rocks. J. Metamorph. Geol., **8**, 191-197.

SEN, S.K. and BHATTACHARYA, A. (1984): An orthopyroxene-garnet thermometer and its application to the Madras charnockites. Contrib. Mineral. Petrol., **88**, 64-71.

SHIBATA, K., YANAI, K. and SHIRAISHI, K. (1986): Rb-Sr whole-rock ages of metamorphic rocks from eastern Queen Maud Land, East Antarctica. Mem. Natl Inst. Polar Res., Spec. Issue, **43**, 133-148.

SHIMURA, T. (1995): Data transmission system from EPMA to the file of spread sheet programs. Geoimformatics, **6**, 31-40.

SHIMURA, T., KOMATSU, M. and IIYAMA, T. (1992): Genesis of the lower crustal Grt-Opx tonalite (S-type) in the Hidaka metamorphic belt, northern Japan. Trans. R. Soc. Edinburgh, **83**, 259-268.

SHIMURA, T., KOMATSU, M., TSUTAI, S., OWADA, M. and TAKAHASHI, Y. (1997): Thermal and Chemical interaction between granitic magmas and wall rocks in the Hidaka metamorphic belt, northern Japan. Mem. Geol. Soc. Jpn., **47**, 1-12.

SHIRAISHI, K., HIROI, Y., MOTOYOSHI, Y. and YANAI, K. (1987): Plate tectonic development of Late Proterozoic paired metamorphic complexes in eastern Queen Maud Land, East Antarctica. Gondwana Six: Structure, Tectonics and Geophysics, ed. by G.D. MCKENZIE. Washington, D.C., Am. Geophys. Union, 309-318 (Geophys. Monogr. Ser. **40**).

SHIRAISHI, K., ELLIS, D.J., HIROI, Y., FANNING, M., MOTOYOSHI, Y. and NAKAI, Y. (1994): Cambrian orogenic belt in East Antarctica and Sri Lanka: implication for Gondwana assembly. J. Geol., **102**, 47-65.

SKJERLIE, K.P., PATIÑO DOUCE, A.E. and JOHNSTON, A.D. (1993): Fluid absent melting of a layered crustal protolith: implications for the generation of anatectic granites. Contrib. Mineral. Petrol., **114**, 365-378.

TAMURA, S., KOBAYASHI, U. and SHUTO, K. (1989): Quantitative analysis of the trace elements in silicate rocks by X-ray fluorescence method. Earth Science (Chikyu Kagaku), **43**, 180-185.

THOMPSON, A.B. (1976a): Mineral reactions in pelitic rocks: I. Prediction of P-T-X (Fe-Mg) phase reactions. Am. J. Sci., **276**, 401-424.

THOMPSON, A.B. (1976b): Mineral reactions in pelitic rocks: II. Calculation of some P-T-X (Fe-Mg) phase reactions. Am. J. Sci., **276**, 425-454.

TODD, V.R. and SHAW, S.E. (1985): S-type granitoids and an I-S line in the Peninsular Ranges batholith, southern California. Geology, **13**, 231-233.

VIELZEUF, D. and HOLLOWAY, R. (1988): Experimental determination of the fluid-absent melting relations in the pelitic system. Consequences for crustal differentiation. Contrib. Mineral. Petrol., **98**, 257-276.

VIELZEUF, D. and MONTEL, J.M. (1994): Partial melting of metagreywackes. Part I. Fluid-absent

experiments and phase relationships. Contrib. Mineral. Petrol., **117**, 375–393.

WHITE, A.J.R. and CHAPPELL, B.W. (1977): Ultrametamorphism and granitoid genesis. Tectonophysics, **43**, 7–22.

WHITE, A.J.R., CLEMENS, J.D., HOLLOWAY, J.R., SILVER, L.T., CHAPPELL, B.W. and WALL, V.J. (1986): S-type granites and their probable absence in southwestern north America. Geology, **14**, 115–118.

YORK, D. (1966): Least-squares fitting of a straight line. Can. J. Phys., **44**, 1079–1086.

(*Received February 2, 1998; Revised manuscript accepted March 17, 1998*)

Table A1. Representative microprobe analyses of garnet in the migmatites.

Sample	BVN06m	BVN06m	BVN46	BVN05-1	BVN05-2
Mineral	Grt	Grt	Grt	Grt	Grt
No.	3.5 (1)	3.5 (3)	21	3	89
	rim	core	core	core	core
SiO2	38.466	38.592	38.152	38.008	37.832
TiO2	0.000	0.000	0.000	0.085	0.017
Al2O3	21.817	21.865	21.187	21.511	21.300
Cr2O3	0.053	0.031	0.047	0.025	0.049
FeO	31.098	30.247	30.487	32.634	33.212
MnO	0.742	0.697	3.275	0.944	0.960
MgO	6.976	7.210	3.759	5.212	4.765
CaO	1.319	1.562	3.672	1.855	1.957
TOTAL	100.471	100.204	100.579	100.274	100.092
Si	2.997	3.004	3.019	3.000	3.003
Ti	0.000	0.000	0.000	0.005	0.001
Al	2.003	2.006	1.976	2.001	1.992
Cr	0.003	0.002	0.003	0.002	0.003
Fe	2.026	1.969	2.018	2.154	2.204
Mn	0.049	0.046	0.220	0.063	0.065
Mg	0.810	0.837	0.444	0.613	0.564
Ca	0.110	0.130	0.311	0.157	0.166
TOTAL	8.000	7.993	7.991	7.994	7.999
O	12	12	12	12	12
X Mg	0.286	0.298	0.180	0.222	0.204
Alm	67.64	66.03	67.44	72.11	73.50
Sps	1.63	1.54	7.34	2.11	2.15
Prp	27.05	28.06	14.82	20.53	18.80
Grs	3.68	4.37	10.41	5.25	5.55

Table A2. Representative microprobe analyses of orthopyroxene in the migmatites.

Sample	BVN03lm	BVN03lm	BVN46	BVN02
Mineral	Opx	Opx	Opx	Opx
No.	28	44	118	48
SiO2	50.051	50.464	50.040	50.185
TiO2	0.065	0.000	0.012	0.000
Al2O3	1.181	1.120	1.060	1.307
Cr2O3	0.000	0.000	0.016	0.000
FeO	32.783	32.805	33.591	32.553
MnO	1.052	1.010	1.095	0.871
MgO	14.103	14.687	13.350	15.016
CaO	0.649	0.365	0.378	0.314
Na2O	0.000	0.000	0.000	0.021
K2O	0.000	0.000	0.000	0.000
P2O5	0.058	0.000	0.000	0.000
BaO	0.022	0.000	0.053	0.000
TOTAL	99.964	100.451	99.595	100.267
Si	1.970	1.973	1.984	1.963
Ti	0.002	0.000	0.000	0.000
Al	0.055	0.052	0.050	0.060
Cr	0.000	0.000	0.001	0.000
Fe	1.079	1.072	1.114	1.065
Mn	0.035	0.033	0.037	0.029
Mg	0.827	0.856	0.789	0.876
Ca	0.027	0.015	0.016	0.013
Na	0.000	0.000	0.000	0.002
K	0.000	0.000	0.000	0.000
P	0.002	0.000	0.000	0.000
Ba	0.001	0.000	0.002	0.000
TOTAL	3.998	4.001	3.992	4.008
O	6	6	6	6
X Mg	0.434	0.444	0.415	0.451
Al/2	0.027	0.026	0.025	0.030

Table A3. Representative microprobe analyses of biotite in the migmatites. The atomic ratios are determined on the basis of the total anion charge number = −44; the general formula is $X_2Y_6Z_8O_{20}(OH)_4$. For the calculation method of anious such as fluorine and chlorine refer to DEER *et al. (1992) page 680. Other formulations are Al^{IV} = 8-Si, Al^{VI} = Al-Al^{IV}, and OH = 4-F-Cl. Mole fractions of each elements are estimated by as following. X-site is each element/(K + Ba + Rb). Y-site is each element/6. Z-site is each element/8. OH-site is each elememt/4.*

Sample	BVN02	BVN02	BVN06m	BVN03lm	BVN03lm	BVN05-2	BVN05-2	BVN46	BVN46	BVN46
Mineral	Bt	Bt	Bt	Bt	Bt	Bt	Bt	Bt	Bt	Bt
No.	6	13	2	24	34	42	46	67	72	76
type	paleo	leuco	melano	leuco	melano	paleo	leuco	leuco	paleo	melano
SiO2	36.647	36.267	36.455	36.874	37.012	36.927	36.163	36.764	37.437	37.254
TiO2	5.785	5.784	5.367	5.746	4.594	5.736	5.703	5.504	5.450	4.488
Al2O3	14.162	14.113	16.274	14.320	14.176	14.724	14.660	14.271	14.447	14.548
Cr2O3	0.001	0.017	0.063	0.043	0.016	0.007	0.000	0.029	0.002	0.029
FeO	22.400	22.631	17.175	21.876	22.017	20.700	22.678	23.717	22.074	21.836
MnO	0.049	0.080	0.000	0.101	0.098	0.000	0.000	0.105	0.125	0.113
MgO	9.096	8.989	12.088	9.689	10.849	9.866	9.091	8.872	9.969	11.137
CaO	0.004	0.014	0.024	0.005	0.004	0.009	0.026	0.022	0.038	0.001
Na2O	0.039	0.043	0.065	0.087	0.062	0.048	0.022	0.066	0.061	0.056
K2O	9.286	9.001	9.485	9.215	9.285	9.539	9.529	9.183	9.253	9.422
NiO	0.000	0.003	0.025	0.049	0.034	0.027	0.068	0.036	0.041	0.044
BaO	0.418	0.436	0.362	0.735	0.736	0.228	0.290	0.360	0.341	0.255
Rb2O	0.101	0.099	0.101	0.086	0.077	0.097	0.097	0.090	0.055	0.095
F	0.463	0.540	0.773	0.701	0.782	0.825	0.742	0.658	0.731	0.868
Cl	0.981	0.944	0.792	0.806	0.806	0.269	0.258	0.702	0.664	0.628
total	99.433	98.962	99.050	100.334	100.549	99.003	99.328	100.380	100.689	100.775
-O=F	-0.195	-0.227	-0.326	-0.295	-0.329	-0.347	-0.312	-0.277	-0.308	-0.366
-O=Cl	-0.221	-0.213	-0.179	-0.182	-0.182	-0.061	-0.058	-0.159	-0.150	-0.142
TOTAL	99.016	98.521	98.545	99.857	100.037	98.594	98.957	99.944	100.231	100.267
Si	5.540	5.518	5.399	5.522	5.539	5.533	5.462	5.526	5.556	5.530
Ti	0.658	0.662	0.598	0.647	0.517	0.646	0.648	0.622	0.608	0.501
Al	2.523	2.531	2.841	2.527	2.500	2.600	2.610	2.528	2.527	2.545
Al^{IV}	2.460	2.482	2.601	2.478	2.461	2.467	2.538	2.474	2.444	2.470
Al^{VI}	0.063	0.048	0.240	0.050	0.039	0.133	0.071	0.054	0.084	0.075
Cr	0.000	0.002	0.007	0.005	0.002	0.001	0.000	0.003	0.000	0.003
Fe	2.832	2.879	2.127	2.740	2.755	2.594	2.864	2.981	2.740	2.711
Mn	0.006	0.010	0.000	0.013	0.012	0.000	0.000	0.013	0.016	0.014
Mg	2.050	2.039	2.669	2.163	2.420	2.204	2.047	1.988	2.206	2.465
Ca	0.001	0.002	0.004	0.001	0.001	0.001	0.004	0.004	0.006	0.000
Na	0.011	0.013	0.019	0.025	0.018	0.014	0.006	0.019	0.018	0.016
K	1.791	1.747	1.792	1.760	1.772	1.823	1.836	1.761	1.752	1.784
Ni	0.000	0.000	0.003	0.006	0.004	0.003	0.008	0.004	0.005	0.005
Ba	0.025	0.026	0.021	0.043	0.043	0.013	0.017	0.021	0.020	0.015
Rb	0.010	0.010	0.010	0.008	0.007	0.009	0.009	0.009	0.005	0.009
F	0.221	0.260	0.362	0.332	0.370	0.391	0.354	0.313	0.343	0.408
Cl	0.251	0.244	0.199	0.205	0.205	0.068	0.066	0.179	0.167	0.158
OH	3.527	3.497	3.439	3.463	3.425	3.541	3.579	3.508	3.490	3.434
O	20.000	20.000	20.000	20.000	20.000	20.000	20.000	20.000	20.000	20.000
X-site	1.837	1.798	1.845	1.838	1.842	1.861	1.873	1.813	1.801	1.824
Y-site	5.609	5.641	5.644	5.623	5.750	5.582	5.639	5.667	5.658	5.775
Z-site	8.000	8.000	8.000	8.000	8.000	8.000	8.000	8.000	8.000	8.000
cation	15.447	15.439	15.489	15.461	15.592	15.443	15.512	15.480	15.459	15.599
OH-site	4.000	4.000	4.000	4.000	4.000	4.000	4.000	4.000	4.000	4.000
TOTAL	39.447	39.439	39.489	39.461	39.592	39.443	39.512	39.480	39.459	39.599
X K	0.975	0.972	0.971	0.958	0.962	0.980	0.980	0.971	0.973	0.978
X Ba	0.013	0.014	0.011	0.023	0.023	0.007	0.009	0.012	0.011	0.008
X Rb	0.005	0.005	0.005	0.005	0.004	0.005	0.005	0.005	0.003	0.005
X Mg	0.420	0.415	0.556	0.441	0.468	0.459	0.417	0.400	0.446	0.476
X Ti	0.117	0.117	0.106	0.115	0.090	0.116	0.115	0.110	0.108	0.087
X Al^{IV}	0.307	0.310	0.325	0.310	0.308	0.308	0.317	0.309	0.305	0.309
X Al^{VI}	0.011	0.009	0.042	0.009	0.007	0.024	0.013	0.010	0.015	0.013
X F	0.055	0.065	0.091	0.083	0.093	0.098	0.089	0.078	0.086	0.102
X Cl	0.063	0.061	0.050	0.051	0.051	0.017	0.017	0.045	0.042	0.040
X OH	0.882	0.874	0.860	0.866	0.856	0.885	0.895	0.877	0.872	0.859

Table A4. Representative microprobe analyses of plagioclase and K-feldspar in the migmatites.

Sample	BVN03lm	BVN06m	BVN46	BVN02	BVN05-1	BVN03lm	BVN46	BVN05-1	BVN05-2
Mineral	Pl	Pl	Pl	Pl	Pl	Kfs	Kfs	Kfs	Kfs
No.	16	77	125	10	87	19	88	6	75
SiO2	61.688	61.397	62.624	60.417	63.386	66.021	66.366	64.920	65.537
TiO2	0.000	0.000	0.000	0.000	0.054	0.000	0.000	0.049	0.000
Al2O3	24.841	24.910	23.952	24.496	23.166	18.789	18.554	18.774	18.892
Cr2O3	0.000	0.000	0.000	0.000	0.000	0.000	0.000	0.015	0.000
FeO	0.015	0.201	0.056	0.000	0.000	0.000	0.000	0.000	0.000
MnO	0.000	0.000	0.000	0.000	0.000	0.007	0.000	0.007	0.000
MgO	0.000	0.000	0.000	0.000	0.000	0.000	0.000	0.000	0.000
CaO	6.446	6.168	5.465	6.452	4.319	0.182	0.151	0.069	0.122
Na2O	7.758	7.747	8.026	7.599	9.118	1.674	1.391	1.905	1.919
K2O	0.035	0.066	0.272	0.373	0.023	12.979	13.046	13.562	12.819
P2O5	0.000	0.050	0.000	0.000	0.000	0.000	0.000	0.000	0.000
BaO	0.000	0.000	0.000	0.000	0.000	0.850	0.099	0.167	0.430
TOTAL	100.783	100.539	100.395	99.337	100.066	100.502	99.607	99.468	99.719
Si	2.715	2.710	2.761	2.705	2.797	3.006	3.027	2.989	2.999
Ti	0.000	0.000	0.000	0.000	0.002	0.000	0.000	0.002	0.000
Al	1.289	1.296	1.245	1.293	1.205	1.008	0.997	1.019	1.019
Cr	0.000	0.000	0.000	0.000	0.000	0.000	0.000	0.001	0.000
Fe	0.001	0.007	0.002	0.000	0.000	0.000	0.000	0.000	0.000
Mn	0.000	0.000	0.000	0.000	0.000	0.000	0.000	0.000	0.000
Mg	0.000	0.000	0.000	0.000	0.000	0.000	0.000	0.000	0.000
Ca	0.304	0.292	0.258	0.310	0.204	0.009	0.007	0.003	0.006
Na	0.662	0.663	0.686	0.660	0.780	0.148	0.123	0.170	0.170
K	0.002	0.004	0.015	0.021	0.001	0.754	0.759	0.796	0.748
P	0.000	0.002	0.000	0.000	0.000	0.000	0.000	0.000	0.000
Ba	0.000	0.000	0.000	0.000	0.000	0.031	0.004	0.006	0.016
TOTAL	4.972	4.973	4.967	4.989	4.989	4.956	4.917	4.986	4.959
O	8	8	8	8	8	8	8	8	8
An	31.40	30.44	26.90	31.25	20.72	0.98	0.83	0.35	0.65
Ab	68.39	69.18	71.50	66.60	79.15	16.23	13.83	17.53	18.42
Or	0.20	0.39	1.59	2.15	0.13	82.79	85.34	82.12	80.94